

# Studies on Density Dependence of Charge Separation in a Direct Energy Converter Using Slanted Cusp Magnetic Field<sup>\*</sup>)

Yoshiro MUNAKATA, Takashi KAWAGUCHI, Hiromasa TAKENO, Yasuyoshi YASAKA, Kazuya ICHIMURA<sup>1)</sup> and Yousuke NAKASHIMA<sup>1)</sup>

*Electrical and Electronic Engineering, Kobe University, 1-1 Rokkodai, Nada, Kobe 657-8501, Japan*

<sup>1)</sup>*Plasma Research Center, University of Tsukuba, 1-1-1 Tennodai, Tsukuba 305-8577, Japan*

(Received 9 December 2011 / Accepted 18 April 2012)

In an advanced fusion, fusion-produced charged particles must be separated from each other for efficient energy conversion to electricity. The CuspDEC performs this function of separation and direct energy conversion. Analysis of working characteristics of CuspDEC on plasma density is an important subject. This paper summarizes and discusses experimental and theoretical works for high density plasma by using a small scale experimental device employing a slanted cusp magnetic field. When the incident plasma is low-density, good separation of the charged particles can be accomplished and this is explained by the theory based on a single particle motion. In high density plasma, however, this theory cannot be always applied due to space charge effects. In the experiment, as gradient of the field line increases, separation capability of the charged particles becomes higher. As plasma density becomes higher, however, separation capability becomes lower. This can be qualitatively explained by using calculations of the modified Störmer potential including space charge potential.

© 2012 The Japan Society of Plasma Science and Nuclear Fusion Research

Keywords: advanced fusion, direct energy conversion, CuspDEC, charge separation, slanted cusp magnetic field, plasma density

DOI: 10.1585/pfr.7.2405071

## 1. Introduction

In D-<sup>3</sup>He fusion power generation, high plant efficiency can be expected by applying direct energy conversion because the majority of the produced energy is kinetic energies of charged particles. Moreover, harmful high energy neutrons are hardly generated, so the D-<sup>3</sup>He fusion power generation is expected as a new excellent power generation method in the economical and environmental aspects. For efficient recovery, particles escaping from the reactor should be separated from each other in energy and electrical polarity. Momota *et al.* proposed a new method of particle separation using a cusp-type direct energy converter (CuspDEC) [1]. Because of the difference of Larmor radius, ions go to point cusp and are separated from electrons going to line cusp.

The authors proposed an application of a slanted cusp magnetic field to CuspDEC to separate charged particles more efficiently and a small scale experimental device was constructed. According to the previous research, good separation of the charged particles can be accomplished and be explained by the theory based on a single particle motion when the incident plasma is low-density [2]. In high density plasma, however, the motion of charged particles is expected to show collective behavior, so the applicability of the theory should be examined. In the previous exper-

iments, the density of the objective plasma is in the order around  $10^{12} \text{ m}^{-3}$ , and this is less than that expected in a real plant of  $10^{16} \text{ m}^{-3}$ . The examination of charge separation in high density plasma was reported [3], but the examined condition was limited. Recent studies of CuspDEC treat two stage deceleration scheme [4], in which an appropriate curvature of magnetic field for energy conversion is necessary. The charge separation in high density plasma should be examined for various curvature conditions.

In this paper, we describe the results of charge separation experiment for dense plasma using our experimental device by employing a helicon wave excited plasma source. Plasma density used in the experiment is from  $10^{13} \text{ m}^{-3}$  to  $10^{15} \text{ m}^{-3}$ . We also examined and discussed about the dependences of plasma density and gradient of the field.

In Sec. 2, the principle theory of charge separation is explained. The experimental device and the way to evaluate separation are explained in Sec. 3. The experimental results and discussion are presented in Sec. 4. The contents of the paper are summarized in Sec. 5.

## 2. Principle Theory

The charge separation using slanted cusp magnetic field can be explained by movable region of incident particles based on Störmer potential [5]. In a system of an axisymmetric magnetic field given by the vector potential  $A_\theta(r, z)$ , the Störmer potential  $F(r, z)$  for particles is repre-

author's e-mail: takeno@eedept.kobe-u.ac.jp

<sup>\*</sup>) This article is based on the presentation at the 21st International Toki Conference (ITC21).

sented by

$$F(r, z) = \frac{m}{2} \left( \frac{p_\theta - qA_\theta(r, z)r}{mr} \right)^2, \quad (1)$$

where  $q$  is the charge,  $m$  is the mass, and  $p_\theta = mr^2\dot{\theta} + qA_\theta r$  is a canonical angular momentum which is conserved in the collision-less system. When initial kinetic energy of the incident particle is  $W = mv_0^2/2$  and no electric field is applied, the particle in a magnetic field can move only in the region satisfying  $F(r, z) \leq W$ . When electric field is applied, its influence also has to be taken into consideration. The Störmer potential is modified and the effective potential  $G$  of the system for a particle at the incident position  $(r_0, z_0)$  with  $v_\theta = 0$  and  $A_\theta(r_0, z_0) = A_0$  is given by

$$G(r, z) = \frac{q^2 A_0^2 r_0^2}{2m r^2} \left( 1 - \frac{r A_0(r, z)}{r_0 A_0} \right)^2 + q\phi(r, z), \quad (2)$$

where  $\phi(r, z)$  is a relative electrostatic potential to that on the incident position (if the potential is 0 on the incident position,  $\phi(r, z)$  directly presents potential to ground). If the initial kinetic energy of particle is lower than  $G$ , it is confined within the potential barrier. In the experimental condition in this paper, the mean free path of electrons is about 13.5 m which is much longer than 1.2 m of the size of the experimental device. Therefore, this experimental environment is a collision-less system, and the principle theory can be applied.

### 3. Experimental Setup

#### 3.1 CuspDEC experimental device

The CuspDEC experimental device is schematically shown in Fig. 1. The device consists of four magnetic coils, four particle collector plates, and a probe.

The coil currents  $I_A$  and  $I_C$ , which have the same direction and value ( $= I_{AC}$ ), create a guide magnetic field. The coil current  $I_B$  is in opposite direction with  $I_{AC}$  and has a different value. The coil D surrounding the plasma source is settled to produce a helicon wave excited plasma. Charged particles are guided to the center of the device (between coils A and B) where a cusp field is created. The field line curvature can be varied from normal to slanted

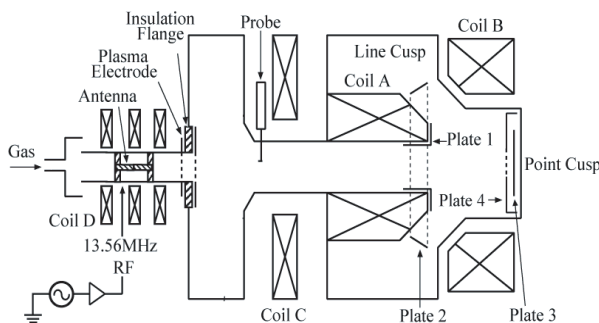


Fig. 1 CuspDEC experimental device.

cusp fields by adjusting the coil currents of  $I_{AC}$  and  $I_B$ , as the radii of coils A and B are different from each other.

At the line cusp side, electron collectors Plate 1 and 2 are settled, and ions collectors Plate 3 and 4, which are usually parallel-connected electrically, are located at the point cusp end. A Langmuir probe located at the entrance is to measure electron density and temperature of the incident plasma.

The incident plasma comes from the plasma source. The electrons are deflected along the field line to the line cusp. These electrons are collected by the particle collectors located at the entrance of line cusp (Plate 1) and the exit of line cusp (Plate 2). On one hand, thermal ions are slightly deflected and separated from electrons. They reach the electrodes located at the inner point cusp (Plate 3) and the outer point cusp (Plate 4). This is because the Larmor radius of ions is far larger compared with that of electrons. Biasing a positive and negative voltage on Plate 3, 4 and 1, 2, respectively, the kinetic energies of ions and electrons are converted into electricity, thus the direct energy conversion is achieved.

#### 3.2 Evaluation of separation efficiency

The motion of electrons is along magnetic field lines, the orbit directly varies with the curvature of the field lines and they reach any particle collectors according to the curvature. The orbit of ions is not sensitive with the curvature and large part of them reaches Plate 3+4 (connected in parallel), so we evaluate the efficiency of charge separation by the amount of electrons arriving at Plate 3+4. We define electron transmission ratio  $R_e$  by the number of electrons arriving at Plate 3+4 divided by the number of incident electrons.

We evaluate  $R_e$  experimentally as follows: most of the field lines at the entrance connect to Plate 3+4 under  $I_B/I_{AC} = 0$ , and the electron currents at Plate 1 and Plate 2 are not detected. Thus, the value of the electron saturation current of Plate 3+4 corresponds to the number of incident electrons. In the same way, the electron saturation current of Plate 3+4 represents the number of electrons on  $I_B/I_{AC} \neq 0$ , so  $R_e$  can be obtained by

$$R_e = \frac{I_{es}(I_B \neq 0)}{I_{es}(I_B = 0)}, \quad (3)$$

where  $I_{es}$  is the electron saturation current of Plate 3+4.

### 4. Experimental Results and Discussion

#### 4.1 Dependence of separation capability on field line curvature and plasma density

In the experiment, argon is used as a material gas of the plasma. Helicon wave excited plasma is used. The incident plasma of the CuspDEC has electron densities from  $10^{13} \text{ m}^{-3}$  to  $10^{15} \text{ m}^{-3}$  and electron temperature around 10 eV.

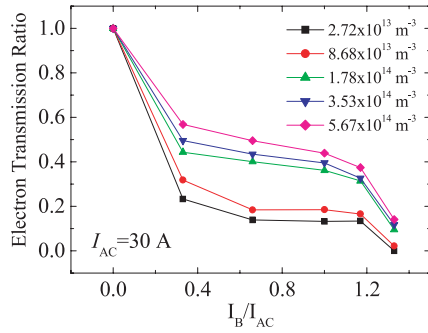


Fig. 2 The dependence of electron transmission ratio on the ratio of magnetic coil currents for several plasma densities.

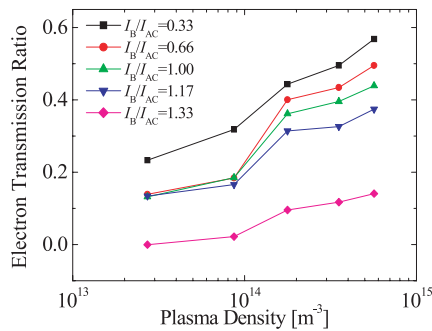


Fig. 3 The dependence of electron transmission ratio on plasma density.

Transmission ratios of electrons  $R_e$  as a function of  $I_B/I_{AC}$  where  $I_{AC} = 30$  A are plotted in Fig. 2 for five cases of the incident plasma density. In all cases of density, reduction of  $R_e$ , which means better charge separation, is found as  $I_B/I_{AC}$  increases.

The experimental results of Fig. 2 are re-plotted in Fig. 3 as a function of plasma density. According to Fig. 3, when the plasma density becomes higher,  $R_e$  becomes larger, which means the degradation of separation. The increment of  $R_e$  is found for all measured conditions of  $I_B/I_{AC}$ .  $R_e$  reaches considerably large values of 0.4-0.6 on high density region except the best condition of  $I_B/I_{AC} = 1.33$ . This is considered to be due to a space potential of ions. As the density increases, density of separated ions remained in the cusp region becomes high resulted in a high space potential. The effect of space potential is discussed in the next section.

## 4.2 Calculation of potential barrier and its variation by stagnant ions

As found in Fig. 2, as the value of  $I_B/I_{AC}$  increases, electron transmission ratio decreases. This variation was obtained on every measured condition, and explained by using calculations of Störmer potential of electrons [6]. Not only in the experimental simulator, but also in an actual device, particle collectors have some biased voltages, thus the electrostatic potential is present, which affects par-

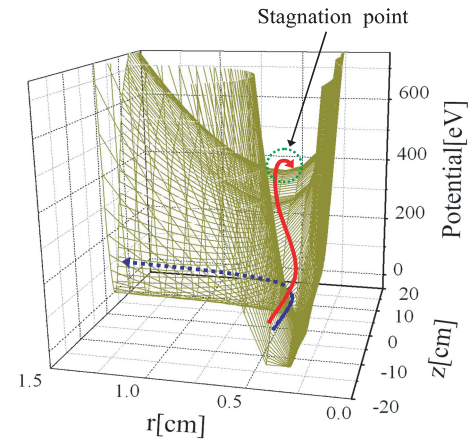


Fig. 4 An example of distribution of  $G$  for an electron on  $I_{AC} = 30$  A,  $I_B = 20$  A, and  $r_0 = 0.3$  cm.

ticle motions. The electron has to ride over  $G$  shown by Eq. (2) to reach the point cusp region.

An example of distribution of  $G$  for an electron on  $I_{AC} = 30$  A and  $I_B = 20$  A is plotted in Fig. 4, where  $(r_0, z_0) = (0.3$  cm,  $-20$  cm). The minimum values are along the field line from the entrance point to the line cusp region as shown by the dashed curve in the figure. The point indicated by the arrow is the stagnation point where the height of the potential barrier to the point cusp is the minimum with a saddle-point-like behavior. The electrons with the initial kinetic energy larger than the value of  $G$  at the stagnation point would ride over the potential barrier and enter into the point cusp region where the ion collectors are located. A schematic trajectory of such a case is depicted in Fig. 4 by the solid curve.

Accordingly, the value of potential at the stagnation point can be important factor for separation of charged particles. Then Störmer potential of electrons was calculated on the same conditions as the experiments and the potential barrier was estimated. When the stagnation point is located beyond Plate 4,  $G$  at Plate 4 is taken as the potential barrier. When the stagnation point is in front of Plate 4, the potential barrier is  $G$  at the stagnation point. The dependence of the potential barrier on the ratio of magnetic coil currents, that is, gradient of the field line is shown in Fig. 5. The bias of Plate 3+4 is 100 V.

According to Fig. 5, as the value of  $I_B/I_{AC}$  increases, the potential barrier increases. Moreover, incident radius becomes larger, the potential barrier increases. This is consistent with experimental results of Fig. 2.

In Fig. 5, however, the potential barrier is too high to be ridden over by electrons. This is because the calculation doesn't contain the potential by stagnant ions in front of the ion collector at the point cusp. When ions go to the point cusp region, they stagnate in front of the ion collector due to deceleration field and create the high positive potential area there. This region is in the cusp field, thus the volume of the plasma is expanded widely and the Debye length

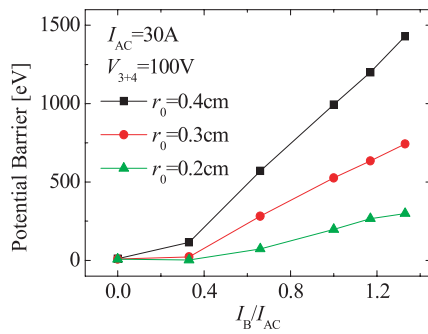


Fig. 5 The dependence of the potential barrier on the ratio of magnetic coil currents.

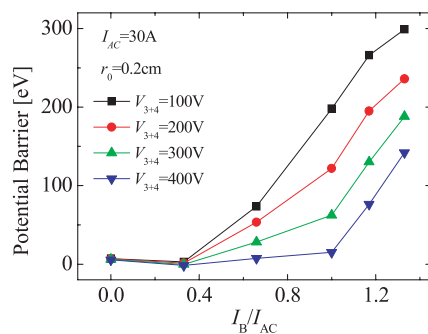


Fig. 6 The dependence of the potential barrier on the bias voltage on Plate 3+4.

is much longer than that of the entrance (several millimeters) and enough for a formation of space potential. This would degrade the potential barrier for electrons. In case of high density plasma, this effect would become large further. We can estimate the effect by the calculation setting a higher bias voltage on Plate 3+4. The same kind of calculation with 100 V to 400 V biasing on Plate 3+4 is shown in Fig. 6, where incident radius is 0.2 cm. In this case, as the bias of Plate 3+4 is increased, the potential barrier for electrons is degraded significantly. This result is consistent with experiments qualitatively. For further detailed discus-

sions, taking account of the behavior of spatial charges is required in the future.

## 5. Summary

Aiming at the practical usage of CuspDEC in an advanced fusion reactor and its two stage deceleration scheme, the characteristics of charge separation by slanted cusp magnetic field for high density plasma were studied.

Even in high density plasma, effect of slanted cusp relatively works well. The results can be explained by the modified Störmer potential including electrostatic potential as the potential barrier to point cusp increases when field curvature increases.

When plasma density becomes high, the value of transmission ratio becomes large, that is, the charge separation is degraded. This is also explained by the modified Störmer potential. As plasma density increases, stagnant ions in front of the collector increase, resulted in the formation of high electrostatic potential. This potential reduces the potential barrier to point cusp, thus the charge separation is degraded. Some schemes recovering potential barrier are needed to be developed.

## Acknowledgments

The authors acknowledge valuable discussions with Drs. Y. Tomita, M. Ishikawa, and I. Katanuma. This work was supported in part by the bilateral coordinated research between Plasma Research Center, University of Tsukuba, National Institute for Fusion Science, and Kobe University.

- [1] H. Momota *et al.*, Proc. 7th Int. Conf. on Emerging Nuclear Energy Systems (1993) p.16.
- [2] T. Yamamoto, Y. Kurumatani, H. Takeno and Y. Yasaka, J. Korean Phys. Soc. **49**, S146 (2006).
- [3] A. Taniguchi, N. Sotani, Y. Yasaka and H. Takeno, J. Plasma Fusion Res. SERIES **9**, 241 (2010).
- [4] Y. Yasaka *et al.*, Trans. Fusion Sci. Technol. **55**, 1 (2009).
- [5] W. Schuuman and H. De Kluiver, Plasma Phys. **7**, 245 (1965).
- [6] Y. Yasaka *et al.*, Nucl Fusion **49**, 075009 (2009).